Int. J. Solids Structures Vol. 28, No. 6, pp. 703–725, 1991
Printed in Great Britain.

0020–7683/91 $3.00 + .00

A BOUNDARY PERTURBATION ANALYSIS FOR ELASTIC INCLUSIONS AND INTERFACES

HUAJIAN GAO
Division of Applied Mechanics, Stanford University, Stanford, CA 94305, U.S.A.

(*Received* 6 *September* 1990; *in revised form* 11 *December* 1990)

Abstract—A first-order boundary perturbation method based on Muskhelishvilli's complex variable representations is formulated for the two-dimensional elasticity problem of a nearly-circular inclusion embedded in an infinite dissimilar material. Universal relations which are independent of loading conditions are established among the solutions for a homogeneous infinite plane, a perfectly-circular inclusion and a slightly-perturbed non-circular inclusion. It is shown that the solution to a circular inclusion can be constructed algebraically from that of an infinite homogeneous plane while the stress distribution along the interface circle leads to the perturbation solutions for a nearly-circular inclusion. Explicit results are given for inclusions with smooth polygon shapes by considering cosine wavy perturbations along a reference circle. A similar analysis is carried out for a bimaterial interface whose shape deviates slightly from a straight line. Our perturbation results can be used to study elastically-induced morphological perturbations of surfaces, interfaces, voids, precipitates and inclusions in a stressed solid. As an example, we demonstrate that, under sufficiently large stresses, material surfaces become unstable against a range of diffusional perturbations bounded by two critical wavelengths. Also, as suggested from our perturbation analysis and verified by a finite element calculation, even slight surface undulation caused by an unstable morphological perturbation can result in substantial stress concentration along the surface, which may cause plastic deformation or brittle fracture before the bulk stress reaches a critical level.

INTRODUCTION

One of the important problems in the micromechanics of solid-state deformation concerns the stress concentration by second-phase inclusions embedded in a dissimilar material. Donnell (1941) seems to have been the first to study the case of an elliptical inclusion in an isotropic matrix. It was later proved by Hardiman (1952) in 2D cases and generalized by Eshelby (1957) to 3D cases that a uniform applied load at infinity induces a constant state of stress within an elliptical or ellipsoidal inclusion. In almost half a century there has been established a vast literature in this area and many useful solutions can be found in Mura's (1987) book. For 2D inclusion problems, the complex variable approach of Muskhelishvilli (1953) for isotropic analysis and that of Stroh (1958) and Lekhnitskii (1981) for anisotropic analysis has frequently been used (e.g. Jaswon and Bhargava, 1961; Bhargava and Radhakrishna, 1964; Sendeckyj, 1970; Berezhnitskii and Denisyuk, 1983; Hwu and Ting, 1989).

It is well known that the development of stresses within a solid may lead to morphological changes. Eshelby (1957) has shown that the total strain energy of a spherical inclusion subject to transformation strains may be lowered by changing the inclusion into less symmetric shapes such as an ellipsoid. Because the sphere has the smallest surface area among all inclusion shapes of a fixed volume, the surface tension tends to resist any morphological changes that would lower the strain energy. Thus, the balance between the elastic energy and the surface energy gives the equilibrium inclusion shape, which is often found to be a nearly circular one. Much of the recent work (e.g. Johnson and Cahn, 1984; Miyazaki *et al.*, 1986; Larala *et al.*, 1989; Kaufman *et al.*, 1989) has indicated that, under a sufficiently-large deviatoric stress state, elastically-misfitting inclusions and precipitates in a solid matrix indeed undergo a shape transition so that an originally-circular inclusion tends to evolve by diffusion processes into a shape of lower symmetry in order to minimize the total free energy in the stressed thermomechanical system. A circular inclusion in the limit of an infinite radius becomes a straight bimaterial interface whose mechanical properties are of growing interest due to rapid advances in composite materials technology. Under sufficiently large stresses, a straight interface may undergo shape transitions into slightly undulating profiles. Srolovitz (1989) has recently shown that, in processes such as

thin-film growth, surface evaporation and condensation, material surfaces under a bulk stress are unstable against diffusional perturbations of sufficiently long wavelengths. Evans and Hutchinson (1989) have pointed out that a non-planar interface morphology has a significant effect on the interface fracture toughness.

In applications such as Ostwald ripening, interface stability and precipitate stability, nucleation and growth, one often needs to consider the mechanics problem of an inclusion or interface with a shape slightly perturbed from a circle or a straight line. However, due to the lack of an efficient analytical approach, most of the research work has to assume an elliptical inclusion shape (e.g. Johnson and Cahn, 1984) or use a boundary integral method (McFadden *et al.*, 1986) which involves heavy numerical computations. In this paper we develop a first-order boundary perturbation analysis for an inclusion whose shape deviates slightly, otherwise arbitrarily, from a reference circle. Based on Muskhelishvilli's (1953) complex variable representations, we analyze a nearly-circular inclusion and a slightly-undulating interface in isotropic solids, deriving perturbation solutions which are accurate to the first order in the deviation of the inclusion shape from a circle or a straight line.

The reference solutions for a perfectly-circular inclusion are essential in our perturbation procedure. By analytic continuation of complex potential functions across the interface circle, it is first shown† that the reference solutions may be directly obtained from those of a homogeneous infinite plane by universal relations which are independent of the loading conditions. The solutions for the deviatoric stress components along the interface are used to construct perturbation solutions for an inclusion with a nearly-circular shape or for an interface with a slightly-wavy profile. Our results may also be specialized to cases such as holes, rigid inclusions, disks and surfaces with shape slightly perturbed from a circle or a straight line. To demonstrate the kind of problems to which the perturbation solutions can be applied, we study in sufficient detail the case of a traction-free surface and show that, under sufficiently-large bulk stresses, a perfectly-flat surface becomes unstable against a range of diffusional perturbations bounded by two critical wavelengths. Given such an intrinsic thermodynamic tendency for surfaces to become rough, further examination indicates that even slight undulation caused by the unstable perturbations can result in substantial stress concentration along the surface, which may then cause plastic deformation or brittle fracture before the bulk stress reaches a critical level. We also perform a finite element calculation for comparison, with results indicating that the perturbation analysis is valid for surface undulations with a moderate magnitude.

COMPLEX VARIABLE REPRESENTATION

Complex potentials in 2D elasticity

In considering the inclusion problems shown in Fig. 1a we will use the following notations for the displacement and stress components in the Cartesian (x, y) and polar (r, θ) coordinates

$$u = u_x + iu_y, \qquad \sigma = \sigma_{xx} + \sigma_{yy} = \sigma_{rr} + \sigma_{\theta\theta}$$
$$\Sigma = \sigma_{yy} - \sigma_{xx} + 2i\sigma_{xy}, \quad \hat{\Sigma} = \sigma_{\theta\theta} - \sigma_{rr} + 2i\sigma_{r\theta} = e^{2i\theta}\Sigma. \tag{1}$$

Apparently, σ denotes the "hydrostatic" part of the stress state while Σ represents the "deviatoric" part whose absolute magnitude gives the value of the maximum shear stress. Following Muskhelishvilli (1953), two complex potentials $\phi(z)$ and $\psi(z)$ can be used to represent the displacement as

$$-2\mu u = -\kappa\phi(z) + z\overline{\phi'(z)} + \overline{\psi(z)} \tag{2}$$

and the stresses as

† After completion of this manuscript, the author found that Honein and Herrmann (1990) have addressed the circular inclusion problem using a similar but more sophisticated method. However, for completeness and for better illustration of the boundary perturbation technique, a brief solution procedure is still preserved in this paper.

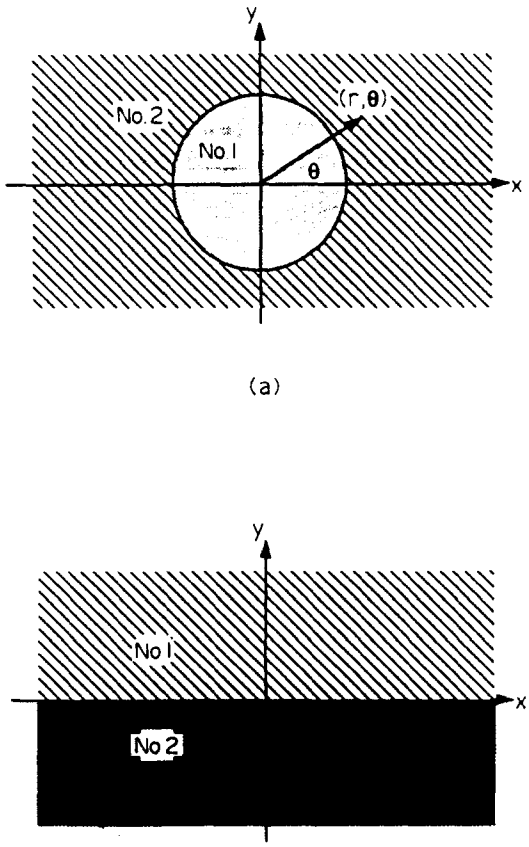

Fig. 1. (a) A circular inclusion No. 1 embedded in a dissimilar material No. 2. (b) A bimaterial interface between Nos 1 and 2.

$$\sigma = 2[\phi'(z) + \overline{\phi'(z)}]$$
$$\Sigma = 2[\bar{z}\phi''(z) + \psi'(z)] \tag{3}$$

where μ and ν are the shear modulus and Poisson ratio respectively; $\kappa = 3-4\nu$ for plane strain and $\kappa = (3-\nu)/(1+\nu)$ for plane stress.

The boundary condition for prescribed traction along a boundary contour $\partial\Omega$ can be written in the form

$$\phi(z) + z\overline{\phi'(z)} + \overline{\psi(z)} = f + \text{constant} \quad \text{on} \quad \partial\Omega \tag{4}$$

where the quantity f is related to the traction t_i by the expression

$$f = \mathrm{i}\int_A^z (t_x + \mathrm{i}t_y)\,\mathrm{d}s \tag{5}$$

which is proportional to the resultant force on an arc from a fixed point A to a variable point z moving along the boundary.

Under a coordinate translation $z_* = z - s$, the complex potentials $\phi_*(z_*)$, $\psi_*(z_*)$ are related to the solutions $\phi(z)$, $\psi(z)$ for the same problem by

$$\phi(z) = \phi_*(z-s), \quad \psi(z) = \psi_*(z-s) - \bar{s}\phi'_*(z-s). \tag{6}$$

Bimaterial mismatch constants

Let an inclusion of material No. 1 be embedded in an otherwise-homogeneous infinite plane of a dissimilar material No. 2. Dundurs (1969) observed that solutions to such bimaterial problems may be expressed via the following two mismatch constants:

$$\alpha = \frac{(\kappa_2+1)/\mu_2 - (\kappa_1+1)/\mu_1}{(\kappa_2+1)/\mu_2 + (\kappa_1+1)/\mu_1}, \quad \beta = \frac{(\kappa_2-1)/\mu_2 - (\kappa_1-1)/\mu_1}{(\kappa_2+1)/\mu_2 + (\kappa_1+1)/\mu_1}. \tag{7}$$

Subscripts 1 and 2 refer to the inclusion No. 1 and the matrix No. 2, respectively. Both α and β vanish when the elastic dissimilarity does. By requiring $-1 < \nu < 1/2$ and $\mu > 0$, it can be shown that α and β are confined to a parallelogram in the (α, β) plane enclosed by $\alpha = \pm 1$ and $\alpha - 4\beta = \pm 1$. For inclusion problems, it is more convenient to use the auxiliary constants Λ, Π, Δ, Ω which are defined as

$$\Lambda = \frac{\alpha+\beta}{1-\beta} = \frac{\kappa_2/\mu_2 - \kappa_1/\mu_1}{1/\mu_2 + \kappa_1/\mu_1}, \qquad \Pi = \frac{\alpha-\beta}{1+\beta} = \frac{1/\mu_2 - 1/\mu_1}{\kappa_2/\mu_2 + 1/\mu_1}$$

$$\Delta = -\frac{\alpha+\beta}{1+\beta} = \frac{\kappa_1/\mu_1 - \kappa_2/\mu_2}{\kappa_2/\mu_2 + 1/\mu_1}, \quad \Omega = -\frac{\alpha-\beta}{1-\beta} = \frac{1/\mu_1 - 1/\mu_2}{\kappa_1/\mu_1 + 1/\mu_2}. \tag{8}$$

These constants are related by $\Delta(\alpha, \beta) = \Lambda(-\alpha, -\beta)$ and $\Omega(\alpha, \beta) = \Pi(-\alpha, -\beta)$. The values of Λ and Π will be interchanged with Δ and Ω when the two materials Nos 1 and 2 are switched. It may be shown that $-1 < \Lambda, \Delta < 3$ and $-1 < \Pi, \Omega < 1$. The constant Π is positive for softer inclusions ($\mu_2 > \mu_1$) but negative for harder inclusions ($\mu_2 < \mu_1$).

CIRCULAR INCLUSIONS

General solution

Consider a perfectly-circular inclusion in $|z| < a$ in a body which is subjected to externally-applied loads and which may also contain various (singularities) defects such as dislocations and transformation strains. When all the singularity points lie outside the inclusion, assume that the potential solutions for an infinite homogeneous plane No. 2 are known as $\phi_\infty(z)$ and $\psi_\infty(z)$ which are analytic in the region $|z| < a$. Under the same loading conditions, let the solutions for a circular inclusion be written as

$$\phi(z) = \phi_\infty(z) + \Phi(z), \quad \psi(z) = \psi_\infty(z) + \Psi(z) \tag{9}$$

where functions $\Phi(z)$ and $\Psi(z)$ represent the "field disturbance" due to the inclusion. We shall attach subscripts 1 and 2 to functions $\phi(z)$, $\psi(z)$ and $\Phi(z)$ and $\Psi(z)$ when inclusion No. 1 and matrix No. 2 are explicitly referred to; for example, $\phi(z)$ will be written as $\phi_1(z)$ in the inclusion region and as $\phi_2(z)$ in the matrix region. Obviously, functions $\Phi_1(z)$, $\Psi_1(z)$ are analytic in the region $|z| < a$ while $\Phi_2(z)$, $\Psi_2(z)$ are analytic in $|z| > a$, which implies the following behavior:

$$\Phi_1(z) = a_0 + a_1 z + a_2 z^2 + \cdots, \quad \Psi_1(z) = b_0 + b_1 z + b_2 z^2 + \cdots \quad (|z| < a)$$

$$\Phi_2(z) = c_1/z + c_2/z^2 + \cdots, \quad \Psi_2(z) = d_1/z + d_2/z^2 + \cdots \quad (|z| > a) \tag{10}$$

in their respective analytic regions.

The traction continuity across the interface $|z| = a$ requires

$$[\![f]\!] = [\![\phi(z)+z\overline{\phi'(z)}+\overline{\psi(z)}]\!] = 0 \tag{11}$$

where $[\![f]\!]$ denotes the jump in quantity f across the interface. Substituting (9) into (11) while replacing $\bar{z}$ by a^2/z along the interface circle $|z| = a$, one may rewrite (11) as

$$\Phi_1(z)+z\Phi_1'\left(\frac{a^2}{z}\right)+\Psi_1\left(\frac{a^2}{z}\right) = \Phi_2(z)+z\Phi_2'\left(\frac{a^2}{z}\right)+\Psi_2\left(\frac{a^2}{z}\right). \tag{12}$$

Following (10), it can be observed that $\Phi_1(z)$, $z\Phi_2'(a^2/z)$, $\Psi_2(a^2/z)$ are analytic in $|z| < a$, while $\Phi_2(z)$, $z[\Phi_1'(a^2/z)-\bar{a}_1]$, $\Psi_1(a^2/z)$ are analytic in $|z| > a$. Subtracting a term $z\bar{a}_1$ $[a_1 = \Phi_1'(0)]$ from both sides of (12), collecting functions which are analytic in $|z| < a$ and $|z| > a$ and using standard procedure of analytic continuation, one finds the relations

$$\begin{aligned}\Phi_1(z) &= z\Phi_2'\left(\frac{a^2}{z}\right)+\Psi_2\left(\frac{a^2}{z}\right)-z\bar{a}_1\\ \Phi_2(z) &= z\left[\Phi_1'\left(\frac{a^2}{z}\right)-\bar{a}_1\right]+\Psi_1\left(\frac{a^2}{z}\right).\end{aligned} \tag{13}$$

Repeating the same procedure for the displacement continuity condition

$$-2[\![u]\!] = \left[\!\!\left[\frac{-\kappa\phi(z)+z\overline{\phi'(z)}+\overline{\psi(z)}}{\mu}\right]\!\!\right] = 0 \tag{14}$$

and using the relations given in (13) leads to

$$\begin{aligned}\Phi_1(z) &= \Lambda\phi_\infty(z)+\Omega z[\bar{a}_1+\bar{\phi}'_\infty(0)]\\ \Phi_2(z) &= \Pi\left[z\bar{\phi}'_\infty\left(\frac{a^2}{z}\right)-z\bar{\phi}'_\infty(0)+\bar{\psi}_\infty\left(\frac{a^2}{z}\right)\right]\end{aligned} \tag{15}$$

where the constants Λ, Π and Ω are given in (8). Differentiating the first of (15) with respect to z and then letting $z = 0$, the unknown constant a_1 is found to be

$$a_1 = \frac{(\Lambda+\Omega^2)\phi'_\infty(0)+\Omega(1+\Lambda)\bar{\phi}'_\infty(0)}{1-\Omega^2}. \tag{16}$$

Combining (13)–(16), the final solutions are obtained as

$$\begin{aligned}\phi_1^0(z) &= (1+\Lambda)\left[\phi_\infty(z)+\frac{\Omega z}{1-\Omega^2}(\bar{\phi}'_\infty(0)+\Omega\phi'_\infty(0))\right]\\ \psi_1^0(z) &= (1+\Pi)\psi_\infty(z)-(\Lambda-\Pi)\frac{a^2}{z}[\phi'_\infty(z)-\phi'_\infty(0)]\\ \phi_2^0(z) &= \phi_\infty(z)+\Pi\left[z\bar{\phi}'_\infty\left(\frac{a^2}{z}\right)-z\bar{\phi}'_\infty(0)+\bar{\psi}_\infty\left(\frac{a^2}{z}\right)\right]\\ \psi_2^0(z) &= \psi_\infty(z)+\Lambda\bar{\phi}_\infty\left(\frac{a^2}{z}\right)+\frac{Ca^2}{z}-\Pi\frac{a^2}{z}\left[\bar{\phi}'_\infty\left(\frac{a^2}{z}\right)-\frac{a^2}{z}\bar{\phi}''_\infty\left(\frac{a^2}{z}\right)-\frac{a^2}{z^2}\bar{\psi}'_\infty\left(\frac{a^2}{z}\right)\right]\end{aligned} \tag{17}$$

where

$$C = \frac{(\Lambda+\Omega)\phi'_\alpha(0)+\Omega(1+\Lambda)\bar{\phi}'_\alpha(0)}{1-\Omega}+\Pi\bar{\phi}'_\alpha(0). \tag{18}$$

Superscript 0 emphasizes that the present solutions are for a perfectly-circular inclusion. It may be verified that the imaginary part of $\phi'_\alpha(0)$ does not affect the stress field. One may sometimes modify $\phi_\alpha(z)$ such that $\phi'_\alpha(0)$ is real and simplify (17), (18) accordingly. The expressions derived in (17), (18) are consistent with those derived by Honein and Herrmann (1990), in slightly different notations. These solutions will be used to construct perturbation solutions for nearly-circular inclusions in the next section. Equations (17) are universal in the sense that they are independent of the loading conditions. Once the problem of a homogeneous infinite plane is solved, the solution to a circular inclusion under the same loading condition can be immediately determined.

For example, in the case of remote loading by uniform stresses σ_{ij}^∞, it is well known that

$$\phi_\alpha(z) = \sigma_\alpha z/4, \quad \psi_\alpha(z) = \Sigma_\alpha z/2 \tag{19}$$

where $\sigma_\alpha = \sigma_{yy}^\infty+\sigma_{xx}^\infty$ and $\Sigma_\alpha = \sigma_{yy}^\infty-\sigma_{xx}^\infty+2i\sigma_{xy}^\infty$. The solutions to a circular inclusion subjected to the same remote loads are obtained from (17) as

$$\phi_1^0(z) = \frac{1+\Lambda}{1-\Omega}\frac{\sigma_\alpha z}{4}, \qquad \psi_1^0(z) = (1+\Pi)\Sigma_\alpha z/2$$

$$\phi_2^0(z) = \frac{1}{4}\left(\sigma_\alpha z+2\Pi\Sigma_\alpha\frac{a^2}{z}\right), \quad \psi_2^0(z) = \frac{1}{2}\left(\Sigma_\alpha z+\frac{\Lambda+\Omega}{1-\Omega}\sigma_\alpha\frac{a^2}{z}+\Pi\Sigma_\alpha\frac{a^4}{z^3}\right) \tag{20}$$

which are consistent with the expressions given in Sendeckyj (1970). A uniform stress state is predicted inside the inclusion as

$$\sigma_1^0 = \frac{1+\Lambda}{1-\Omega}\sigma_\alpha, \quad \Sigma_1^0 = (1+\Pi)\Sigma_\alpha. \tag{21}$$

The stresses along the inclusion boundary in the matrix region are

$$\sigma_2^0 = \mathrm{Re}\,[\sigma_\alpha-2\Pi\Sigma_\alpha e^{-2i\theta}], \quad \Sigma_2^0 = \Sigma_\alpha-\Pi\Sigma_\alpha e^{-4i\theta}-\frac{\Lambda+\Omega}{1-\Omega}\sigma_\infty e^{-2i\theta}. \tag{22}$$

For uniaxial tension when $\sigma_{yy}^\infty = \sigma_\alpha = \Sigma_\alpha = T$, the hoop stresses along $|z| = a$ are

$$\sigma_{1\theta\theta}^0 = \frac{1}{2}\left[\frac{1+\Lambda}{1-\Omega}+(1+\Pi)\cos 2\theta\right]T, \quad \sigma_{2\theta\theta}^0 = \frac{1}{2}\left[1-\frac{\Lambda+\Omega}{1-\Omega}+(1-3\Pi)\cos 2\theta\right]T. \tag{23}$$

While the maximum of $\sigma_{1\theta\theta}^0$ always occurs at $\theta = 0$, $\sigma_{2\theta\theta}^0$ is maximized at $\theta = 0$ when $-1 < \Sigma < 1/3$ (softer or slightly-harder inclusions) but at $\theta = \pi/2$ when $1/3 < \Pi < 1$ (much-harder inclusions).

The universal relations (17) can be also used to study, for example, a dislocation at a position $s = x_d+iy_d$ with Burgers vector $b = b_x+ib_y$ interacting with an inclusion. The solution for a straight dislocation in an infinite body is

$$\phi'_\alpha(z) = \frac{\mu b}{\pi i(\kappa+1)(z-s)}, \quad \psi'_\alpha(z) = \frac{\mu}{\pi i(\kappa+1)(z-s)}\left(-\bar{b}+\frac{\bar{s}b}{z-s}\right). \tag{24}$$

In applying (17) to (24), one needs to take the logarithmic branch cut of $\ln(z-s)$ to be outside the inclusion region so that $\phi_\alpha(z)$ and $\psi_\alpha(z)$ are analytic within $|z| < a$.

If all the singularity points lie within the inclusion region, the corresponding formulae may be derived following similar steps from (9) to (18). Letting $\phi_\infty(z)$ and $\psi_\infty(z)$ now denote the solutions for a homogeneous infinite plane of material No. 1 which are analytic in $|z| > a$, it can be shown that the inclusion solutions are (also see Honein and Herrmann, 1990)

$$\phi_1^0(z) = \phi_\infty(z) + \Omega\left[z\bar{\phi}'_\infty\left(\frac{a^2}{z}\right) + \bar{\psi}_\infty\left(\frac{a^2}{z}\right)\right] + \frac{\Omega^2(c+\Omega\bar{c})}{1-\Omega^2}z$$

$$\psi_1^0(z) = \psi_\infty(z) + \Delta\bar{\phi}_\infty\left(\frac{a^2}{z}\right) + \Omega\frac{a^2}{z}\left\{\bar{c} - \phi'_\infty\left(\frac{a^2}{z}\right) + \frac{a^2}{z^2}\left[z\bar{\phi}''_\infty\left(\frac{a^2}{z}\right) + \bar{\psi}'_\infty\left(\frac{a^2}{z}\right)\right]\right\}$$

$$\phi_2^0(z) = (1+\Delta)\phi_\infty(z)$$

$$\psi_2^0(z) = (1+\Omega)\psi_\infty(z) - (\Delta-\Omega)\frac{a^2}{z}\phi'_\infty(z) + \frac{\Omega(\bar{c}+\Omega c)}{1-\Omega}\frac{a^2}{z} \tag{25}$$

where

$$c = \lim_{z\to\infty}\frac{z}{a^2}\psi_\infty(z). \tag{26}$$

One may show that c must be real when the total moment vanishes on a closed contour surrounding the inclusion region $|z| < a$.

As an example of this case, consider that the inclusion is subjected to a stress-free transformation strain ε_{ij}^T in the sense of Eshelby (1957). Letting

$$\sigma^T = \frac{\mu_1}{\kappa_1+1}(\varepsilon_{xx}^T + \varepsilon_{yy}^T)$$

$$\Sigma^T = \frac{\mu_1}{\kappa_1+1}(\varepsilon_{yy}^T - \varepsilon_{xx}^T + 2i\varepsilon_{xy}^T) \tag{27}$$

it is known that (e.g. Jaswon and Bhargava, 1960)

$$\phi_\infty(z) = -\sigma^T z, \qquad \psi_\infty(z) = -\Sigma^T z \qquad \text{in} \quad |z| < a$$

$$\phi_\infty(z) = -\Sigma^T\frac{a^2}{z}, \quad \psi_\infty(z) = -2\sigma^T\frac{a^2}{z} - \Sigma^T\frac{a^4}{z^3} \quad \text{in} \quad |z| > a. \tag{28}$$

Substituting these into (25) immediately yields

$$\phi_1^0(z) = -\frac{1+\Omega}{1-\Omega}\sigma^T z, \qquad \psi_1^0(z) = -(1+\Delta)\Sigma^T z$$

$$\phi_2^0(z) = -(1+\Delta)\Sigma^T\frac{a^2}{z}, \quad \psi_2^0(z) = -2\frac{1+\Omega}{1-\Omega}\sigma^T\frac{a^2}{z} - (1+\Delta)\Sigma^T\frac{a^4}{z^3}. \tag{29}$$

Comparing (29) and (20) with (28) suggests that under remote loading $(\sigma_\infty, \Sigma_\infty)$ and the transformation strain (σ^T, Σ^T), the effect of the non-homogeneous inclusion is equivalent to an effective transformation strain given by

$$\sigma_{\text{eff}}^T = -\frac{\sigma_\infty}{4}\frac{\Lambda+\Omega}{1-\Omega} + \sigma^T\frac{1+\Omega}{1-\Omega}, \quad \Sigma_{\text{eff}}^T = -\Sigma_\infty\Pi/2 + \Sigma^T(1+\Delta) \tag{30}$$

in a completely-homogeneous material. This is consistent with the concept of "equivalent inclusion" introduced by Eshelby (1957).

The universal relations (25) require that the functions $\phi_\infty(z)$ and $\psi_\infty(z)$ be analytic in $|z| > a$. This may not be true if there exists a net Burgers vector or net resultant force within the inclusion since in those cases logarithmic functions appear in $\phi_\infty(z)$ and $\psi_\infty(z)$ and have branch cuts going to infinity. However, one may solve such problems by first differentiating the displacement and traction continuity conditions with respect to z so that only the derivatives of $\phi_\infty(z)$ and $\psi_\infty(z)$ are involved in the analytic continuation procedure. We do not pursue the details here.

Special cases: circular holes and disks

The following two special cases can be considered.

(i) *An infinite plane with a circular hole or rigid inclusion.* In the case of a circular hole one has $\mu_1 = 0$, $\alpha = \Lambda = \Pi = -1$ so that (17) reduces to $\phi_1^0(z) = \psi_1^0(z) = 0$ and

$$\phi_2^0(z) = \phi_\infty(z) - \left[z\bar{\phi}'_\infty\left(\frac{a^2}{z}\right) - z\bar{\phi}'_\infty(0) + \bar{\psi}_\infty\left(\frac{a^2}{z}\right)\right]$$

$$\psi_2^0(z) = \psi_\infty(z) - \bar{\phi}_\infty\left(\frac{a^2}{z}\right) - \frac{a^2}{z}[\phi'_\infty(0) + \bar{\phi}'_\infty(0)]$$

$$+ \frac{a^2}{z}\left[\bar{\phi}'_\infty\left(\frac{a^2}{z}\right) - \frac{a^2}{z}\bar{\phi}''_\infty\left(\frac{a^2}{z}\right) - \frac{a^2}{z^2}\bar{\psi}'_\infty\left(\frac{a^2}{z}\right)\right]. \tag{31}$$

This relation has been derived by Honein and Herrmann (1988). Similarly, the solution for *a rigid circular inclusion* can be obtained by setting relevant constants in (17) as $\mu_1 = \infty$, $\alpha = 1$, $\Lambda = 1/\Pi = \kappa_2$ and $\Omega = -1$.

(ii) *A circular disk.* To specialize (25) to a circular disk by letting $\mu_2 = 0$ and $\Delta = \Omega = -1$, one must enforce the condition that there is no net resultant force or moment on the disk. This condition requires that the constant c of (25) be real so that one has $\phi_2^0(z) = \psi_2^0(z) = 0$ and

$$\phi_1^0(z) = \phi_\infty(z) - \left[z\bar{\phi}'_\infty\left(\frac{a^2}{z}\right) + \bar{\psi}_\infty\left(\frac{a^2}{z}\right)\right] + \tfrac{1}{2}cz$$

$$\psi_1^0(z) = \psi_\infty(z) - \bar{\phi}_\infty\left(\frac{a^2}{z}\right) - \frac{a^2}{z}\left\{c - \phi'_\infty\left(\frac{a^2}{z}\right) + \frac{a^2}{z^2}\left[z\bar{\phi}''_\infty\left(\frac{a^2}{z}\right) + \bar{\psi}'_\infty\left(\frac{a^2}{z}\right)\right]\right\}. \tag{32}$$

A straight interface

The case of a straight interface between two dissimilar materials (Fig. 1b) may be viewed as an inclusion with an infinite radius. Assuming that all the singularities lie in region No. 2 so that $\phi_\infty(z)$, $\psi_\infty(z)$ are the solutions for a homogeneous infinite plane of No. 2, it may be shown that the solutions to the straight interface are

$$\phi_1^0(z) = (1+\Lambda)\phi_\infty(z)$$

$$\phi_2^0(z) = \phi_\infty(z) + \Pi[z\bar{\phi}'_\infty(z) + \bar{\psi}_\infty(z)]$$

$$\psi_1^0(z) = (1+\Pi)\psi_\infty(z) - (\Lambda - \Pi)z\phi'_\infty(z)$$

$$\psi_2^0(z) = \psi_\infty(z) + \Lambda\bar{\phi}_\infty(z) - \Pi z[\bar{\phi}'_\infty(z) + z\bar{\phi}''_\infty(z) + \bar{\psi}'_\infty(z)]. \tag{33}$$

Similar relations in slightly different notations can be found in Suo (1989) and Honein and Herrmann (1990). When the singularities lie within No. 1, the same relations hold when replacing Λ, Π with Δ, Ω and reinterpreting $\phi_\infty(z)$, $\psi_\infty(z)$ as the solutions to an infinite plane of No. 1.

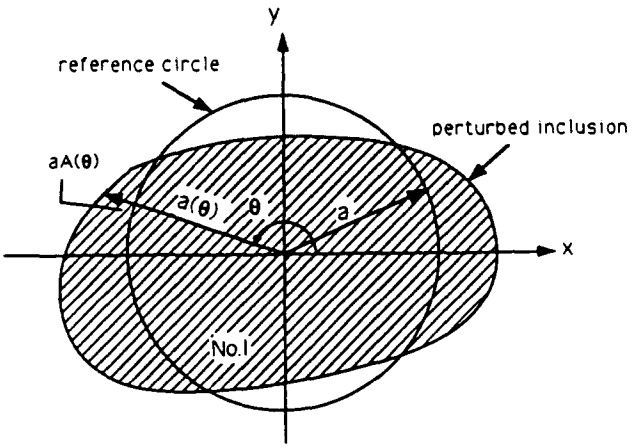

Fig. 2. A nearly-circular inclusion whose shape $a(\theta)$ deviates slightly from a reference circle of radius a.

BOUNDARY PERTURBATION: NEARLY-CIRCULAR INCLUSIONS

General solution

We have shown that the solution to a circular inclusion can be obtained from that of a homogeneous infinite plane via the universal relations given in (17), (25). Based on the solutions for a circular inclusion, we will develop a first-order perturbation analysis for nearly-circular inclusions whose shapes may deviate slightly, but otherwise arbitrarily, from a circle.

Figure 2 shows an inclusion bounded by a contour Γ which differs slightly from a reference circle of radius a so that a point z on Γ at a polar angle θ can be written as

$$z = [1 + A(\theta)]a\,e^{i\theta} \tag{34}$$

where the real quantity $A(\theta) \ll 1$† gives the perturbation magnitude at the given position θ. The actual inclusion shape is described by $r = a(\theta) = a[1 + A(\theta)]$ which may be viewed as being perturbed from the reference circle at $|z| = a$ by a small perturbation $aA(\theta)$.

Equation (34) can be alternatively written as

$$z = \zeta[1 + A(\zeta)], \qquad \zeta = a\,e^{i\theta} \tag{35}$$

where ζ moves along the reference circle $|\zeta| = a$. Let the solutions for the reference circular inclusion be expressed in terms of the potentials $\phi^0(z)$ and $\psi^0(z)$. The traction and displacement due to $\phi^0(z)$ and $\psi^0(z)$ are continuous across $|\zeta| = a$ so that

$$[\![\phi^0(\zeta) + \zeta\overline{\phi^{0\prime}(\zeta)} + \overline{\psi^0(\zeta)}]\!] = 0, \qquad \left[\!\!\left[\frac{-\kappa\phi^0(\zeta) + \zeta\overline{\phi^{0\prime}(\zeta)} + \overline{\psi^0(\zeta)}}{\mu}\right]\!\!\right] = 0. \tag{36}$$

Differentiating the above with respect to ζ while noting that $\bar{\zeta} = a^2/\zeta$ yields

$$\left[\!\!\left[\frac{-\kappa\phi^{0\prime}(\zeta) + \overline{\phi^{0\prime}(\zeta)}}{\mu}\right]\!\!\right] = \left[\!\!\left[\frac{e^{-2i\theta}\,[\zeta\overline{\phi^{0\prime\prime}(\zeta)} + \overline{\psi^{0\prime}(\zeta)}]}{\mu}\right]\!\!\right] = \frac{a^2}{\zeta^2}\left[\!\!\left[\frac{\Sigma^0}{\mu}\right]\!\!\right] \tag{37}$$

where Σ^0 is the solution for the deviatoric stress components along the reference circular inclusion, such as those given in (21), (22) under remote-loading conditions.

The solution to the actual inclusion shape may be written in a perturbation form

† The perturbation magnitude is magnified in Fig. 2 for illustration.

$$\phi(z) = \phi^0(z) + \Phi(z), \quad \psi(z) = \psi^0(z) + \Psi(z) \tag{38}$$

where, in subscripted notation, $\Phi_1(z)$ and $\Psi_1(z)$ are analytic in the inclusion while $\Phi_2(z)$ and $\Psi_2(z)$ are analytic in the matrix, admitting the same asymptotic behaviors as in (10).

The same traction and displacement continuity conditions (11), (14) must hold along the inclusion boundary Γ. As a point z along Γ is perturbed to the reference position ζ by (35), $\phi(z)$ and $\psi(z)$ are perturbed as

$$\phi(z) = \phi^0(\zeta) + A(\zeta)\zeta\phi^{0\prime}(\zeta) + \Phi(\zeta), \quad \psi(z) = \psi^0(\zeta) + A(\zeta)\zeta\psi^{0\prime}(\zeta) + \Psi(\zeta). \tag{39}$$

Substituting (39) into (11), (14), using (37) and neglecting higher-order terms lead to

$$\begin{aligned} [\![\Phi(\zeta) + \zeta\overline{\Phi'(\zeta)} + \overline{\Psi(\zeta)}]\!] &= -A(\zeta)\bar{\zeta}[\![\Sigma^0]\!] \\ \left[\!\!\left[\frac{-\kappa\Phi(\zeta) + \zeta\overline{\Phi'(\zeta)} + \overline{\Psi(\zeta)}}{\mu}\right]\!\!\right] &= -A(\zeta)\bar{\zeta}\left[\!\!\left[\frac{\Sigma^0}{\mu}\right]\!\!\right]. \end{aligned} \tag{40}$$

Thus, to within first-order accuracy, the problem of a nearly-circular inclusion is equivalent to a perfectly-circular inclusion with some "prescribed" displacement and traction discontinuity across the interface. Apparently, only the deviatoric part of the stress distribution along the interface affects the perturbation field.

Noting that the traction continuity for the reference inclusion requires $[\![\sigma_{rr}^0]\!] = 0$ and $[\![\sigma_{r\theta}^0]\!] = 0$, eqns (40) can be rearranged into the following more convenient form:

$$\begin{aligned} \Phi_1(\zeta) - \Omega[\zeta\Phi_1'(\zeta) + \Psi_1(\zeta)] - (1+\Lambda)\Phi_2(\zeta) &= \Omega A(\zeta)\bar{\zeta}\Sigma_1^0 \\ \Phi_2(\zeta) - \Pi[\zeta\Phi_2'(\zeta) + \Psi_2(\zeta)] - (1+\Delta)\Phi_1(\zeta) &= \Pi A(\zeta)\bar{\zeta}\Sigma_2^0. \end{aligned} \tag{41}$$

The unknown functions $\Phi_1(z)$, $\Psi_1(z)$, $\Phi_2(z)$ and $\Psi_2(z)$ can be determined from the above equations following the method of Muskhelishvilli (1953). For example, applying the operator

$$\frac{1}{2\pi i}\oint_{|\zeta|=a}\frac{d\zeta}{\zeta - z} \tag{42}$$

for $|z| < a$ to the first of (41) and using the expansion (10) lead to

$$\Phi_1(z) = \frac{\Omega}{2\pi i}\oint_{|\zeta|=a}\frac{A(\zeta)\bar{\zeta}\Sigma_1^0}{\zeta - z}\,d\zeta + \Omega[\bar{a}_1 z + 2\bar{a}_2 + \bar{b}_0]. \tag{43}$$

Recall that $a_1 = \Phi_1'(0)$. Differentiating the above once with respect to z, letting $z = 0$ on both sides and making variable transformation $\zeta = a\,e^{i\theta}$, one obtains

$$a_1 - \Omega\bar{a}_1 = \frac{\Omega}{2\pi}\int_0^{2\pi} A(\theta)\bar{\Sigma}_1^0(\theta)\,e^{-2i\theta}\,d\theta. \tag{44}$$

The unknown constant a_1 is then found to be

$$a_1 = \frac{\Omega}{1-\Omega^2}\frac{1}{2\pi}\int_0^{2\pi} A(\theta)[\bar{\Sigma}_1^0(\theta)\,e^{-2i\theta} + \Omega\Sigma_1^0(\theta)\,e^{2i\theta}]\,d\theta. \tag{45}$$

Applying the same operator in (42) for $|z| > a$ to the second of (41) gives

$$\Phi_2(z) = -\frac{\Pi}{2\pi i}\oint_{|\zeta|=a}\frac{A(\zeta)\zeta\bar{\Sigma}_2^0}{\zeta - z}\,d\zeta. \tag{46}$$

Taking the complex conjugate of (41) and repeating the above procedure leads to the determination of $\Psi_1(z)$ and $\Psi_2(z)$. Noting that constant terms in the potential functions do not affect the stress field and hence can be dropped, it is finally found that

$$\Phi_1(z) = \frac{\Omega}{2\pi i}\oint_{|\zeta|=a}\frac{A(\zeta)\zeta\bar{\Sigma}_1^0}{\zeta - z}\,d\zeta + \Omega\bar{a}_1 z$$

$$\Phi_2(z) = -\frac{\Pi}{2\pi i}\oint_{|\zeta|=a}\frac{A(\zeta)\zeta\bar{\Sigma}_2^0}{\zeta - z}\,d\zeta \tag{47}$$

and

$$\Psi_1(z) = -\frac{1}{2\pi i}\oint_{|\zeta|=a}\frac{A(\zeta)\zeta\Sigma_1^0}{\zeta - z}\,d\zeta + \frac{1+\Pi}{\Pi}\Phi_2\left(\frac{a^2}{z}\right) - \frac{a^2}{z}[\Phi_1'(z) - a_1]$$

$$\Psi_2(z) = \frac{1}{2\pi i}\oint_{|\zeta|=a}\frac{A(\zeta)\zeta\Sigma_2^0}{\zeta - z}\,d\zeta + \frac{1+\Omega}{\Omega}\Phi_1\left(\frac{a^2}{z}\right) - \frac{a^2}{z}\Phi_2'(z) \tag{48}$$

where a_1 is given by (45). Far away from the inclusion, the potentials behave as $1/z$ and the stressed decay as $1/r^2$. The final solutions for a nearly circular inclusion are obtained by combining (47), (48) with the reference solutions for a perfectly-circular inclusion that may be derived from (17), (25). Such a perturbation procedure can be immediately carried out once the inclusion shape $a(\theta)$ $(= a[1 + A(\theta)])$ and the reference solutions Σ_1^0, Σ_2^0 are known. In the Appendix we show that the general solutions given in (47), (48) may be used to develop integral formulae for calculating stresses along the inclusion boundary.

Cosine wavy inclusion boundaries

It is interesting to consider inclusions with the following cosine shape function:

$$a(\theta) = a_0(1 + A\cos n\theta) \tag{49}$$

where a_0, A are real constants with $A \ll 1$. The case $n = 1$ corresponds to a rigid translation of the circle $r = a_0$ by amount A in the x direction and $n = 2$ corresponds to slightly squeezing the circle into an ellipse. The above cosine function can also simulate polygon shapes with smoothed corners for $n \geqslant 3$. As shown in Fig. 3, the polygon shapes are best approximated by (49) when the curvature is required to vanish at the most concave locations where $\cos n\theta = -1$, corresponding to having

$$A = 1/(1 + n^2). \tag{50}$$

The fact that $A \leqslant 0.1$ when $n \geqslant 3$ indicates that the polygon shapes given by (49), (50) represent small perturbations from a circle, and suggests use of the boundary perturbation formula (47), (48) for determining the stress solutions.

For simplicity, we shall only consider the case of remote loading so that the reference solutions Σ_1^0 and Σ_2^0 are those given in (21), (22) which may be rewritten as

$$\Sigma_1^0 = (1 + \Pi)\Sigma_\infty, \quad \Sigma_2^0 = \Sigma_\infty - \Pi\bar{\Sigma}_\infty\frac{a^4}{\zeta^4} - \frac{\Lambda + \Omega}{1 - \Omega}\sigma_\infty\frac{a^2}{\zeta^2}. \tag{51}$$

Substituting the cosine wavy perturbation

$$a(\theta)=1+\cos n\theta/(1+n^2)$$

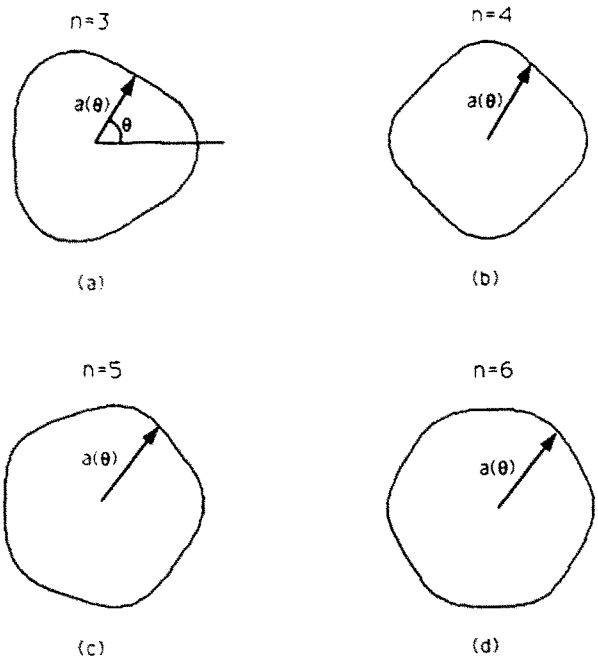

Fig. 3. Smooth polygonal shapes simulated by cosine wavy inclusion shapes: (a) $n = 3$: equilateral triangle; (b) $n = 4$: square; (c) $n = 5$: pentagon; (d) $n = 6$: hexagon.

$$A(\zeta) = \frac{A}{2}\left(\frac{\zeta^n}{a^n} + \frac{a^n}{\zeta^n}\right) \tag{52}$$

and the reference solutions (51) into (47), (48), and then carrying out the contour integrations by the Cauchy integration theorem leads to the final solutions for any wavenumber n. We summarize the results as follows:

(i) *Translation mode* n = 1. In this case, it may be shown that the perturbation solutions can be simply written as

$$\phi(z) = \phi^0(z-A), \quad \psi(z) = -A\phi^{0\prime}(z-A)+\psi^0(z-A) \tag{53}$$

within first-order accuracy in A, where $\phi^0(z)$ and $\psi^0(z)$ are given by (20). Comparing with (6) reveals that the above solution simply states that the $n = 1$ mode represents a rigid translation of the circular inclusion by A in the x direction which is equivalent to a coordinate translation to $z_* = z - A$.

(ii) *Elliptical mode* n = 2. In this case we find

$$\phi_1(z) = \frac{z}{4}\left[\frac{1+\Lambda}{1-\Omega}\sigma_\infty + \frac{2A\Omega(1+\Pi)}{1-\Omega^2}(\bar{\Sigma}_\infty + \Omega\Sigma_\infty)\right]$$

$$\psi_1(z) = \frac{z}{2}\left[(1+\Pi)\Sigma_\infty - \frac{A(1+\Pi)(\Lambda+\Omega)}{1-\Omega}\sigma_\infty\right]$$

$$\phi_2(z) = \phi_2^0(z) + \frac{A\Pi}{2}\left(\Sigma_\infty\frac{a^4}{z^3} - \frac{\Lambda+\Omega}{1-\Omega}\sigma_\infty\frac{a^2}{z}\right)$$

$$\psi_2(z) = \psi_2^0(z) + \frac{Aa^2}{2z}\left[\Pi\bar{\Sigma}_\infty\left(-\frac{\Lambda+\Omega}{1-\Omega}+4\frac{a^4}{z^4}\right)+\Sigma_\infty\frac{\Pi+\Omega}{1-\Omega}+\frac{(1-\Pi)(\Lambda+\Omega)}{1-\Omega}\sigma_\infty\frac{a^2}{z^2}\right]. \tag{54}$$

These solutions are just the first-order expansion in A of the exact solutions for an elliptical inclusion which have been explicitly listed in Sendeckyj (1970).

(iii) *Polygon mode* n $\geqslant 3$. The following solutions may be derived for inclusions with a smooth polygon shape:

$$\phi_1(z) = \frac{z}{4}\left[\frac{1+\Lambda}{1-\Omega}\sigma_\infty + 2A\Omega(1+\Pi)\bar{\Sigma}_\infty\left(\frac{z}{a}\right)^{n-2}\right]$$

$$\psi_1(z) = \frac{(1+\Pi)z}{2}\left\{\Sigma_\infty - A\left[\frac{\Lambda+\Omega}{1-\Omega}\sigma_\infty\left(\frac{z}{a}\right)^{n-2} + \Pi\Sigma_\infty\left(\frac{z}{a}\right)^{n-4}\right.\right.$$

$$\left.\left. + \Omega(n-1)\bar{\Sigma}_\infty\left(\frac{z}{a}\right)^{n-4} - \frac{\Omega}{1-\Omega^2}(\bar{\Sigma}_\infty + \Omega\Sigma_\infty)\left(\frac{z}{a}\right)^2\right]\right\}$$

$$\phi_2(z) = \phi_2^0(z) + \frac{A\Pi}{2}\frac{a^2}{z}\left[\bar{\Sigma}_\infty\left(\frac{a}{z}\right)^n - \frac{\Lambda+\Omega}{1-\Omega}\sigma_\infty\left(\frac{a}{z}\right)^{n-2} - \Pi\Sigma_\infty\left(\frac{a}{z}\right)^{n-4}\right]$$

$$\psi_2(z) = \psi_2^0(z) - \frac{A}{2}\frac{a^2}{z}\left\{\Sigma_\infty[1-(1-\Omega)(1+\Pi)+\Pi^2(n-3)]\left(\frac{a}{z}\right)^{n-2}\right.$$

$$\left. - \frac{\Lambda+\Omega}{1-\Omega}\sigma_\infty[1-(n-1)\Pi]\left(\frac{a}{z}\right)^n - \Pi(n+2)\bar{\Sigma}_\infty\left(\frac{a}{z}\right)^{n+2}\right\}. \tag{55}$$

These solutions may be used to study the perturbation effects of smooth polygonal inclusions such as a cuboid when $n = 4$.

Of course, the general perturbation formulae derived here may be specialized to slightly-perturbed circular holes and disks in the limiting moduli cases. However, we do not pursue the details here.

A SLIGHTLY-UNDULATING INTERFACE BETWEEN TWO DISSIMILAR MATERIALS

The same perturbation procedure may be applied to study a slightly-undulating interface (Fig. 4) between two semi-infinite dissimilar materials Nos 1 and 2. The shape of the interface differs slightly from a straight line, which is described by the following perturbation

$$z = t + iA(t) \tag{56}$$

where t denotes a point on the reference straight interface along the real x axis and $y = A(x)$

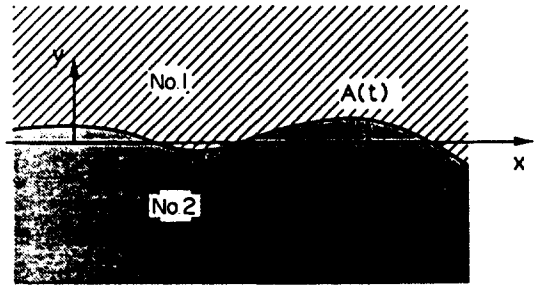

Fig. 4. A slightly-undulating interface which is perturbed from a straight line by $A(t)$.

gives the undulating profile of the actual interface. Substituting the first-order perturbation expressions

$$\phi(z) = \phi^0(z) + \Phi(z) = \phi^0(t) + \mathrm{i}A(t)\phi^{0\prime}(t) + \Phi(t)$$
$$\psi(z) = \psi^0(z) + \Psi(z) = \psi^0(t) + \mathrm{i}A(t)\psi^{0\prime}(t) + \Psi(t) \tag{57}$$

into the displacement and traction continuity conditions (11), (14) yields two equations

$$\Phi_1(t) - \Omega[t\bar{\Phi}_1'(t) + \bar{\Psi}_1(t)] - (1+\Lambda)\Phi_2(t) = -\mathrm{i}\Omega A(t)\bar{\Sigma}_1^0(t)$$
$$\Phi_2(t) - \Pi[t\bar{\Phi}_2'(t) + \bar{\Psi}_2(t)] - (1+\Delta)\Phi_1(t) = -\mathrm{i}\Pi A(t)\bar{\Sigma}_2^0(t) \tag{58}$$

for determining the unknown perturbation functions $\Phi_1(z)$, $\Psi_1(z)$, $\Phi_2(z)$ and $\Psi_2(z)$. Here $\phi^0(z)$ and $\psi^0(z)$ denote the reference solutions for a perfectly-straight interface as shown in Fig. 1b. Applying the operator

$$\frac{1}{2\pi\mathrm{i}}\int_{-\infty}^{\infty}\frac{\mathrm{d}t}{t-z} \tag{59}$$

for $\mathrm{Im}[z] > 0$ to the first of (58) and for $\mathrm{Im}[z] < 0$ to the second of (58), then repeating the same for their complex conjugates, lead to the final solutions

$$\Phi_1(z) = -\frac{\Omega}{2\pi}\int_{-\infty}^{\infty}\frac{A(t)\bar{\Sigma}_1^0(t)}{t-z}\,\mathrm{d}t$$
$$\Phi_2(z) = \frac{\Pi}{2\pi}\int_{-\infty}^{\infty}\frac{A(t)\bar{\Sigma}_2^0(t)}{t-z}\,\mathrm{d}t$$
$$\Psi_1(z) = -\frac{1}{2\pi}\int_{-\infty}^{\infty}\frac{A(t)\bar{\Sigma}_1^0(t)}{t-z}\,\mathrm{d}t + \frac{1+\Pi}{\Pi}\Phi_2(z) - z\Phi_1'(z)$$
$$\Psi_2(z) = \frac{1}{2\pi}\int_{-\infty}^{\infty}\frac{A(t)\bar{\Sigma}_2^0(t)}{t-z}\,\mathrm{d}t + \frac{1+\Omega}{\Omega}\Phi_1(z) - z\Phi_2'(z). \tag{60}$$

For example, consider a wavy interface with wavelength λ and amplitude A so that

$$A(t) = A\cos kt \tag{61}$$

where $k = 2\pi/\lambda$. Assume that the reference stress distributions along the straight interface are uniform. Carrying out the contour integrations in (60) by the Cauchy residue theorem, one finds

$$\phi_1(z) = \sigma_1^0 z/4 - \frac{\mathrm{i}A}{2}\Omega\bar{\Sigma}_1^0\,\mathrm{e}^{\mathrm{i}kz}$$
$$\psi_1(z) = \Sigma_1^0 z/2 - \frac{\mathrm{i}A}{2}[\Sigma_1^0 - (1+\Pi)\Sigma_2^0 - \Omega\mathrm{i}kz\bar{\Sigma}_1^0]\,\mathrm{e}^{\mathrm{i}kz}$$
$$\phi_2(z) = \sigma_2^0 z/4 - \frac{\mathrm{i}A}{2}\Pi\bar{\Sigma}_2^0\,\mathrm{e}^{-\mathrm{i}kz}$$
$$\psi_2(z) = \Sigma_2^0 z/2 - \frac{\mathrm{i}A}{2}[\Sigma_2^0 - (1+\Omega)\Sigma_1^0 - \Pi\mathrm{i}kz\bar{\Sigma}_2^0]\,\mathrm{e}^{-\mathrm{i}kz} \tag{62}$$

which gives the stress field as

$$\sigma_1 = \sigma_1^0 + 2A\Omega k\, e^{-ky}\, \mathrm{Re}\,[\bar{\Sigma}_1^0 e^{ikx}]$$
$$\Sigma_1 = \Sigma_1^0 + Ak\, e^{-ky}\,[\Sigma_1^0 - \Omega\bar{\Sigma}_1^0 + 2iy\Omega k\bar{\Sigma}_1^0 - (1+\Pi)\bar{\Sigma}_2^0]\, e^{ikx}$$
$$\sigma_2 = \sigma_2^0 - 2A\Pi k\, e^{ky}\, \mathrm{Re}\,[\bar{\Sigma}_2^0 e^{-ikx}]$$
$$\Sigma_2 = \Sigma_2^0 - Ak\, e^{ky}\,[\Sigma_2^0 - \Pi\bar{\Sigma}_2^0 + 2iy\Pi k\bar{\Sigma}_2^0 - (1+\Omega)\bar{\Sigma}_1^0]\, e^{-ikx}. \quad (63)$$

Observe that the perturbation effect decays exponentially in the form of $e^{-2\pi|y|/\lambda}$ at positions away from the interface.

STABILITY AND STRESS ANALYSIS OF SURFACES OF A STRESSED SOLID

Morphological instabilities along a surface

To demonstrate the kind of applications our perturbation solutions can be used for, we examine a traction-free surface under a lateral bulk stress T as shown in Fig. 5. Letting $\mu_1 = 0$, $\Lambda = \Pi = -1$, $\sigma_1^0 = \Sigma_1^0 = 0$ and $\sigma_2^0 = -\Sigma_2^0 = \sigma_{2xx}^0 = T$ in (63) gives the first-order solutions for a cosine wavy surface as

$$\sigma_2 = T(1 - 2Ak\, e^{ky}\cos kx), \quad \Sigma_2 = -T[1 - 2Ak\, e^{ky}(1 - ky)\, e^{-ikx}] \quad (64)$$

which match the solutions derived by Srolovitz (1989) and Gao (1991a) via different approaches. In particular, the tangential stress along the surface is predicted as

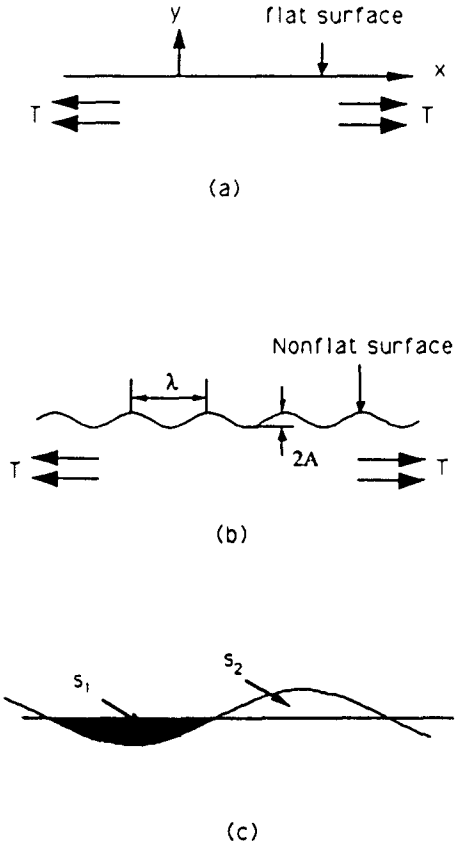

Fig. 5. (a) A perfectly-flat surface of a stressed solid; (b) a slightly-undulating surface; (c) transport of mass in the process of surface diffusion from the configuration of (a) to that of (b).

$$\sigma_{11}(x) = T\left(1 - \frac{4\pi A}{\lambda}\cos\frac{2\pi x}{\lambda}\right). \tag{65}$$

In view of the physical possibility of diffusional mass transport along a material surface, a fundamental stability question can be posed, namely: is a perfectly-flat plane surface (Fig. 5a) stable, i.e. is the plane surface energetically the most preferred configuration for any stress T? If not, what is the stability condition, i.e. what are the critical values of T? The perturbation results we derived here can be used to investigate the stability issue by considering the total energy change associated with a small wavy perturbation along the surface (Fig. 5b). The strain energy variation for the shape change of a traction-free surface was studied by Rice and Drucker (1967). In one period $0 < x < \lambda$, one may write

$$\delta U = \int_0^\lambda w(x)\delta A(x)\,\mathrm{d}x \tag{66}$$

where $\delta A(x)$ is an infinitesimal surface perturbation and $w(x)$ is the strain energy density function along the surface. The stress distribution given in eqn (65) for a wavy surface results in the following strain energy density along the surface:

$$w(x) = \frac{\kappa+1}{16\mu}\sigma_{11}^2(x) = \frac{(\kappa+1)T^2}{16\mu}\left(1 - \frac{8\pi A}{\lambda}\cos\frac{2\pi x}{\lambda}\right) + O(A^2). \tag{67}$$

In the more general case, the strain energy variation due to an arbitrary perturbation along a bimaterial interface can be found in Eshelby (1970).

Let a wavy surface with current amplitude A be subjected to an additional infinitesimal perturbation $\delta A\cos(2\pi x/\lambda)$. This is equivalent to enlarging the wave amplitude from A to $A+\delta A$. Replacing the $\delta A(x)$ in eqn (66) by $\delta A\cos(2\pi x/\lambda)$, dividing both sides of (66) by δA, then letting δA approach zero, one finds the rate of change of strain energy in one period ($0 < x < \lambda$) as

$$\frac{\partial U}{\partial A} = \int_0^\lambda w(x)\cos\frac{2\pi x}{\lambda}\,\mathrm{d}x = -\frac{(\kappa+1)T^2}{4\mu}\pi A + O(A^2). \tag{68}$$

Equation (68) suggests that the strain energy is actually lowered by enlarging the wave amplitude A, corresponding to enlarging the perturbation. This provides a fundamental mechanism for driving initially-flat surfaces into an undulating morphology via diffusional mass transport. Let the wavy surface shown in Fig. 5b be viewed as being perturbed incrementally, by integrating infinitesimal perturbations δA, from the perfectly-flat configuration when $A = 0$ to the current wave amplitude A. In this process, the total strain energy change is calculated by integrating the derivative (68), giving

$$\Delta U = \int_0^A \frac{\partial U}{\partial A}\,\mathrm{d}A = -\frac{(\kappa+1)T^2}{8\mu}\pi A^2 + O(A^3). \tag{69}$$

Thus the energy change due to the perturbation is of order A^2. In the same process, the surface energy and possibly the gravitational potential energy are also subjected to variations. Consider the total energy change in one period of the wavy perturbation. The surface energy change is proportional to the increase in the surface area, i.e.

$$\Delta E_s = \gamma\int_0^\lambda \{\sqrt{1+[A'(x)]^2} - 1\}\,\mathrm{d}x = \gamma A^2\pi^2/\lambda \tag{70}$$

where the material constant γ is the specific surface energy of the solid. This consideration

is analogous to the well-known argument by Griffith (1921) in considering the balance between the strain energy release and surface energy change in a brittle fracture process.

The wavy perturbation involves transport of mass from the shaded area S_1 to another area S_2 (Fig. 5c), which may result in a net change ΔE_g in the gravitational potential energy. Such a change may be significant in applications such as the topological undulation along the Earth's surface due to tectonic stresses. It is elementary to show that

$$\Delta E_g = \rho g \lambda A^2/4 \tag{71}$$

where ρ, g denote, respectively, the material density and the gravity constant. Summing all the terms in eqns (69)–(71) yields the overall energy change as

$$\Delta E_{tot} = \frac{1}{\lambda}\left\{\gamma\pi^2 - \frac{(\kappa+1)\pi T^2}{8\mu}\lambda + \frac{\rho g}{4}\lambda^2\right\}A^2 + O(A^3). \tag{72}$$

If the quadratic expression within the curly bracket (as a coefficient of A^2) is always positive, a perfectly-flat surface would be stable against all perturbations, in the sense that any change in surface profile will result in an increase in the total energy of the system. Define two material constants

$$\hat{\lambda} = 2\pi\sqrt{\gamma/\rho g}, \quad \hat{T} = \sqrt{\frac{8\mu}{\kappa+1}}(\rho g \gamma)^{1/4}. \tag{73}$$

The stability condition can be written as

$$T < \hat{T} \tag{74}$$

which ensures that there are no real roots for the quadratic function in eqn (72). When the stability condition (74) is violated, two real and positive roots emerge as

$$\lambda_{1,2} = \hat{\lambda}(T/\hat{T})^2[1 \pm \sqrt{1-(\hat{T}/T)^4}]. \tag{75}$$

The surface is then found to be unstable against perturbations between λ_1 and λ_2. Thus the two critical wavelengths λ_1 and λ_2 provide an instability range in which surface morphology bears the tendency to become rough. It is clear from (72) that perturbations with very small and very large wavelengths are stable since for small λ the surface tension term dominates, and for large λ the gravity term dominates. When the stress exceeds the critical level $\hat{T}$, material surfaces will tend to undulate in a non-planar configuration. In a similar vein, it can be shown (work in progress) that bimaterial interfaces under various loading conditions may exhibit the same type of tendency toward roughness. Evans and Hutchinson (1989) have pointed out that the non-planarity along an interface has a significant effect on the interface fracture toughness.

Table 1 lists values of $\hat{T}$ and $\hat{\lambda}$ for a number of materials. It is found that $\hat{\lambda}$ is of the order of 1 cm and $\hat{T}$ is of the order of 1 MPa. When the bulk stress level T is close to $\hat{T}$, the critical wavelengths are in the order of 1 cm. This length scale is sufficiently large that

Table 1

	γ (J m^{-2})	μ (Pa)	σ_Y (Pa)	ρ (kg m^{-3})	$\hat{T}$ (Pa)	$\hat{\lambda}$ (m)
Ag	1.14	3.38×10^{10}	—	10.5×10^{3}	5.99×10^{6}	0.021
Al	0.98	2.65×10^{10}	1.4×10^{8}	2.7×10^{3}	3.616×10^{6}	0.038
Au	1.485	3.10×10^{10}	—	19.32×10^{3}	7.48×10^{6}	0.018
Cu	1.725	5.46×10^{10}	3.1×10^{8}	8.96×10^{3}	7.93×10^{6}	0.028
Fe	1.95	8.6×10^{10}	2.8×10^{8}	7.87×10^{3}	9.7×10^{6}	0.032
Ni	2.28	9.47×10^{10}	–	8.9×10^{3}	10.8×10^{6}	0.032
W	2.80	16.0×10^{10}	4.1×10^{8}	19.3×10^{3}	17.96×10^{6}	0.024

one would expect observations of the morphological instabilities along a surface to be routine. However, we find that the value of $\hat{T}$ exceeds (by order of 10) the yield stress for all the materials listed in Table 1. Thus, assuming that under normal conditions the bulk stress is limited to the yield stress, the effect of gravity would prohibit the surface morphological changes. While in most engineering structures the stress level is below $\hat{T}$, for applications such as thin films on substrate the stress level can be as large as 1 GPa. As T is increased from $\hat{T}$, the critical wavelength λ_1 approaches infinity while λ_2 quickly assumes the value

$$\lambda_c = \frac{\hat{\lambda}\hat{T}^2}{2T^2} = \frac{8\pi\mu\gamma}{(\kappa+1)T^2} \tag{76}$$

which is independent of the gravity constant. In fact, λ_2 is within 1% of λ_c once $T/\hat{T} > 2$. Thus, as far as the micro-level surface morphology is concerned, the gravitational energy terms can be ignored in the stability analysis. The critical wavelength λ_c has been obtained by Srolovitz (1989) using a different approach by considering the detailed process of surface diffusion driven by the gradient of chemical potential along a perturbed surface. Srolovitz (1989) also showed that the most unstable perturbation mode occurs at $\lambda_m = (4/3)\lambda_c$. Since the driving force per unit surface area for diffusion is proportional to $-\Delta E_{tot}/\lambda$ and the diffusion process involves transport of mass in an area of order $A\lambda$ over a distance λ (Fig. 5c), one may justify that the most unstable perturbation mode corresponds to maximizing the quantity $-\Delta E_{tot}/\lambda^3$. Using the material constants provided in Table 1, it may be verified that for stresses in the giga Pascal range, the values λ_c and λ_m are in the nanometer (10^{-9} m) range. This is consistent with the reported values (Berger *et al.*, 1988) on the island-like growth along the surface of an InGaAs film on GaAs substrate where the stress within the film can be as large as 5.8 GPa due to a 3% lattice mismatch and the island spacing is observed to be of the order of 6 nm.

Stress concentration at slightly-undulating surfaces

Given the intrinsic undulating tendency of a stressed surface described above, it is necessary to examine the stress concentration effects caused by the undulation. Following (65), the maximum stress concentration occurs at the wave troughs such as $x = \lambda/2$ where

$$\sigma_{max} = T\left(1 + \frac{4\pi A}{\lambda}\right) + O(A^2). \tag{77}$$

The remarkable fact is: the ratio A/λ affects the magnitude of the stress concentration by a constant coefficient equal to $4\pi = 12.566$, suggesting that slight perturbations can magnify the bulk stress T easily by a factor of 2 or 3. For example, an undulating surface with $A/\lambda = 0.1$ magnifies the bulk stress by roughly 2.25. This value is only approximate, but it has been verified by a finite element calculation (to be described shortly) to be within 8% accuracy. It is thus expected that the micro-level bumps and troughs can result in a significant stress concentration along the surface. The stress concentration may lead to mechanical failures along the surface and may have more consequences for piezoelectric materials where the deformation is coupled to an applied electric field. Using an approach based on properties of elastic Green's functions, Gao (1991a) has also shown that the 3D problem of a biaxially-stressed non-planar surface exhibits a similar level of stress concentration.

The kind of stability and stress analyses illustrated above, which may also be carried out for general bimaterial interfaces and inclusion problems, has significant implications for modern technological innovations. For example, layered semiconductor thin-film structures with different lattice parameters have found numerous applications in the development of electronic and optical devices. The lattice mismatch creates strain which results in the formation of dislocations and cracks in the structure. The nucleation of dislocations is also observed in thin-film structures that comprise integrated circuit and magnetic disks. It is of

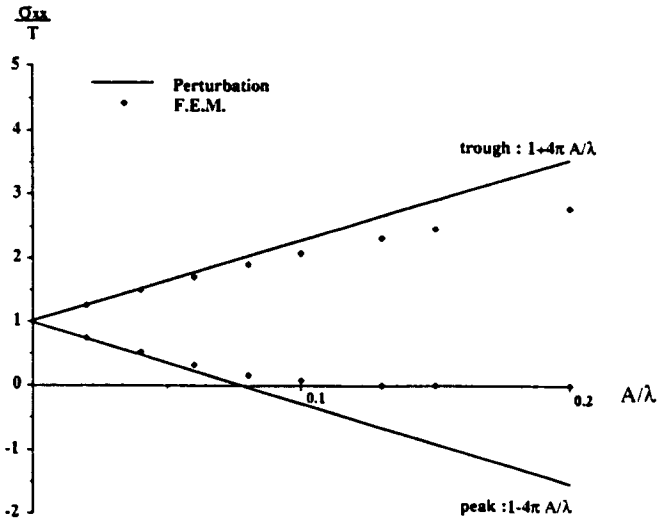

Fig. 6. The stress concentration along a wavy surface: perturbation solutions versus FEM results at a wave trough and a wave peak.

extremely-high technological importance to reduce the dislocation densities to manufacture high-performance, high-yield electronic devices. Nix (1989) has recently reviewed some of the mechanical properties of thin films on substrates, and pointed out that very large stresses (e.g. 0.5 GPa), generated by strain sources such as thermal mismatch and epitaxial lattice mismatch, may be present to cause plastic deformation and fracture. Under such high stresses, a slight magnification of the bulk stress by surface or interface perturbations such as micro-level bumps and troughs is likely to play a role in triggering nucleation processes of dislocations and cracks. Assume that the surface morphology of the thin films displays slight undulations at the micro level with $A/\lambda = 0.1$. Our perturbation result (77) then suggests that the surface stress may be magnified to a level around 1 GPa, much higher than the bulk stress value. Therefore, at least in highly-stressed thin films, the surface morphology can play an important role in activating formation of dislocations and cracks. Once formed, these surface flaws can cause significant strength degradation and malfunction of semiconductor devices, sometimes even leading to ultimate structural failure before the bulk stress reaches a critical level. Our stability study may eventually suggest methods to control surface and interface morphology in manufacturing processes to achieve desired mechanical properties for thin-film devices.

FEM calculation

To examine the range of validity of the perturbation results, we have performed a finite element calculation for the wavy surface shown in Fig. 5b. The stress concentration factor is computed, for different ratios of A/λ, at the wave peaks and troughs where minimum and maximum stress occurs. The symmetry condition $u_x = 0$ is imposed at a wave trough or peak during calculation. We use an 8-noded isoparametric Lagrangian element with an intensively-refined mesh near the surface regions. Figure 6 shows the FEM results compared with the perturbation solutions. At a wave trough, the perturbation solution $1+4\pi(A/\lambda)$ for the maximum stress concentration is found to be within 8% of the FEM data for $A/\lambda < 0.1$ and within 20% for $A/\lambda < 0.2$. For surfaces with $A/\lambda = 0.1$, the FEM analysis shows a maximum stress concentration of 2.07 (compared to the perturbation result 2.25). At a wave peak, the perturbation solution $1-4\pi(A/\lambda)$ becomes negative when $A/\lambda > 0.08$, while the FEM analysis indicates that the stress quickly approaches zero for $A/\lambda > 0.1$.

SUMMARY AND CONCLUSIONS

The main results of the present work are:

(a) Analytic continuation has been used to derive universal relations given in eqns (17)

and (25) between the elastic solutions for a circular inclusion and those for a homogeneous infinite plane under the same loading conditions. These relations are universal in the sense that they are independent of the loading conditions. The solution to a circular inclusion problem can thus be immediately obtained from that for a homogeneous infinite plane.

(b) Based on Muskhelishvilli's complex variable representations, general perturbation formulae [equations (38), (47), (48)] valid for arbitrary loading conditions are established for an inclusion whose shape deviates slightly, otherwise arbitrarily, from that of a reference circular inclusion. The complex potential functions for the actual inclusion are determined from the distribution of the deviatoric stress components for the reference circular inclusion. Based on the general formulae, explicit solutions are given for inclusions with smooth polygon shapes (Fig. 3) under remote loads by considering a cosine wavy perturbation along a reference circle.

(c) A similar perturbation analysis has been carried out for an interface whose shape deviates slightly, otherwise arbitrarily, from a straight line. The general formulae which are given in eqn (60) have also been specialized to consider a cosine wavy interface profile, with results indicating that the perturbation effects decay exponentially at a distance away from the interface.

(d) To demonstrate the kind of applications to which our perturbation analysis can be applied, we study in sufficient detail a traction-free surface under a laterally-applied bulk stress and show that, under sufficiently-large stresses, material surfaces become unstable against a range of morphological perturbations bounded by two critical wavelengths given by (75). Also, it is suggested from the perturbation analysis and verified by a finite element calculation (Fig. 6) that even slight surface undulations may result in significant stress concentrations, which in highly-stressed solids may cause surface fracture or plastic deformation before the bulk stress reaches a critical level.

(e) Integral formulae which involve principal value integrations in the Cauchy sense are developed in the Appendix for calculating the stress distribution along a perturbed inclusion boundary.

The methodology developed here may also be applied to an elastic medium coupled to other external fields such as piezoelectric materials and thermoelastic and poroelastic solids. It is of high technological value to understand the effect of the surface and interface morphology of these materials, and hopefully by that understanding one may find ways of controlling the interface diffusion mechanism by means of prescribed thermomechanical processes.

Acknowledgements—The work reported was supported by NSF under the Research Initiation Grant No. MSS9008521 and by the NSF-MRL program through the Center for Material Research at Stanford University. Mr Jin Lee's contribution in carrying out the finite element calculation leading to results presented in Fig. 6 is gratefully acknowledged.

REFERENCES

Berezhnitskii, L. T. and Denisyuk, I. T. (1983). Plane problems for an anisotropic body with a sharp-ended anisotropic inclusion. *Sov. Mat. Sci.* **19**, 135–142.

Berger, P. R., Chang, K., Bhattacharya, P. and Singh, J. (1988). Role of strain and growth conditions on the growth front profile of $In_xGa_{1-x}As$ on GaAs during the pseudomorphic growth regime. *Appl. Phys. Lett.* **53**, 684–686.

Bhargava, R. D. and Radhakrishna, H. C. (1964). *J. Phys. Soc. Japan* **19**, 396–405.

Donnell, L. H. (1941). Stress concentration due to elliptical discontinuities in plates under edge stresses. In *Theodore Von Karman Anniversary Volume*, pp. 293–309. California Institute of Technology, CA.

Dundurs, J. (1969). Elastic interactions of dislocations with inhomogeneities. In *Mathematical Theory of Dislocations*, pp. 70–115. American Society of Mechanical Engineering, New York.

Eshelby, J. D. (1957). The determination of the elastic field of an ellipsoidal inclusion, and related problems. *Proc. R. Soc.* **A241**, 376–396.

Eshelby, J. D. (1970). Energy relations and the energy-momentum tensor in continuum mechanics. In *Inelastic Behavior of Solids* (Edited by M. F. Kanninen), pp. 78–115. McGraw-Hill, Scarborough, CA.

Evans, A. G. and Hutchinson, J. W. (1989). Effects of non-planarity of the mixed mode fracture resistance of bimaterial interfaces. *Acta Metall.* **37**, 55–91.

Gao, H. (1991a). Stress concentration at slightly undulating surfaces. *J. Mech. Phys. Solids* (MS 320).

Gao, H. (1991b). Stress analysis of smooth polygonal holes via a boundary peturbation method. *J. Appl. Mech.*, in press.
Griffith, A. A. (1921). The phenomena of rupture and flow in solids. *Philosoph. Trans. R. Soc. London* **A221**, 163–197.
Hardiman, N. J. (1952). Elliptical elastic inclusions in an infinite elastic plate. *Q. J. Mech. Appl. Math.* **7**, 226–230.
Honein, T. and Herrmann, G. (1988). The involution correspondence in plane elastostatics for regions bounded by a circle. *J. Appl. Mech.* **55**, 566–573.
Honein, T. and Herrmann, G. (1990). On bonded inclusions with circular or straight boundaries in plane elastostatics. *J. Appl. Mech.*, **57**, 850–856.
Hwu, C. and Ting, T. C. T. (1989). Two dimensional problems of the anisotropic solid with an elliptical inclusion. *Q. J. Mech. Appl. Math.* **42**, 553–572.
Jaswon, M. A. and Bhargava, R. D. (1960). Two-dimensional elastic inclusion problems. *Proc. Camb. Phil. Soc.* **57**, 669–680.
Johnson, W. C. and Cahn, J. W. (1984). Elastically induced shape bifurcations pf inclusions. *Acta Metall.* **32**, 1925–1933.
Kaufman, M. J., Voorhee, P. W., Johnson, W. C. and Biancaniello, F. S. (1989). Elastically induced morphological instabilities of a misfitting precipitate. *Metall. Trans. A (Physical Metallurgy and Materials Science)*, **20A**, 2171–2175.
Larala, V. J., Johnson, W. C. and Voorhee, P. W. (1989). Kinetics of Ostwald ripening in stressed solid : the lower volume fraction limit. *Scripta Metall.* **23**, 1749–1754.
Lekhnitskii, S. G. (1981). *Theory of Elasticity on an Anisotropic Body*. MIR, Moscow.
McFadden, G. B., Voorhees, P. W., Boisvert, R. F. and Meiron, D. I. (1986). Boundary integral method for the simulation of two-dimensional particle coarsening. *J. Sci. Comput.* **1**, 117–144.
Miyazaki, Seki, K., Doi, M. and Kozakai, T. (1986). Stability bifurcations in the coarsening of precipitates in elastically constrained systems. *Mat. Sci. Engng* **77**, 125–132.
Mura, T. (1987). *Micromechanics of Defects in Solids*. Martinus Nijhoff, Boston.
Muskhelishvilli, N. I. (1953). *Some basic problems of the mathematical theory of elasticity*. Noordhoff, Groningen.
Nix, W. D. (1989). Mechanical properties of thin films. 1988 Institute of Metals Lecture, Stanford, CA.
Rice, J. R. (1989). Weight function theory for three-dimensional elastic crack analysis. In *Fracture Mechanics: Perspectives and Directions (Twentieth Symp.)*, ASTM STP 1020 (Edited by R. P. Wei and R. P. Gangloff), pp. 29–57. American Society for Testing and Materials, Philadelphia.
Rice, J. R. and Drucker, D. C. (1967). Energy changes in stressed bodies due to void and crack growth. *Int. J. Fracture Mech.* **3**, 19–27.
Sendeckyj, G. P. (1970). Elastic inclusion problems in plane elasticity. *Int. J. Solids Structures* **6**, 1535–1543.
Sokolnikoff, I. S. (1983). *Mathematical Theory of Elasticity*. Krieger, Florida.
Srolovitz, D. J. (1989). On the stability of surfaces of stressed solids. *Acta Metall.* **37**, 621–625.
Stroh, A. N. (1958). Dislocations and cracks in anisotropic elasticity. *Philosoph. Mag.* **7**, 625–646.
Suo, Z. (1989). Singularities interacting with interfaces and cracks. *Int. J. Solids Structures* **25**, 1133–1142.

APPENDIX: INTEGRAL FORMULAE FOR STRESS DISTRIBUTION ALONG A PERTURBED INCLUSION BOUNDARY

Based on the general perturbation formulae given in (47), (48) for a nearly-circular inclusion and those given in (60) for a slightly-undulating interface, one may derive explicit integral formulae for calculating the stress distribution along the inclusion boundary where the perturbation effect is most significant.

To avoid any problems of singular perturbations in directly calculating the stress distribution along the inclusion bondary Γ at a chosen polar position α, we shall choose the reference circle to be located at $|z| = a(\alpha)$ so that $A(\theta = \alpha) = 0$ at the chosen α where the field quantities will be calculated (Fig. A1). The importance of such a treatment will become self-evident shortly. For a given inclusion shape $r = a(\theta)$, the perturbation $A(\theta)$ is thus taken to be

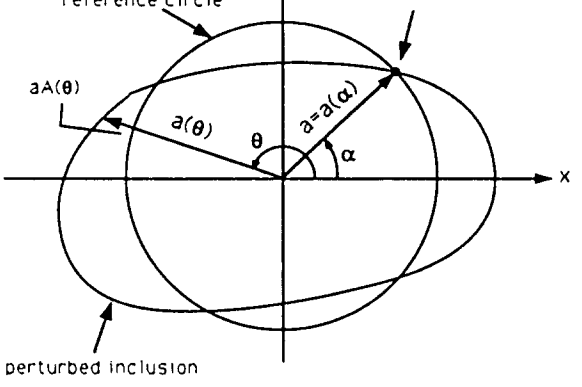

Fig. A1. Relocation of the reference circle at an observation point α.

$$A(\theta) = \frac{a(\theta) - a(\alpha)}{a(\alpha)}, \quad A'(\alpha) = \frac{a'(\alpha)}{a(\alpha)}. \tag{A1}$$

For conciseness, we shall let a stand for $a(\alpha)$ in the following calculations.

Using (47), consider the derivative term

$$\Phi_1'(z) = \frac{\Omega}{2\pi i} \oint_{|\zeta|=a} \frac{A(\zeta)\zeta\bar{\Sigma}_1^0}{(\zeta - z)^2} \, d\zeta + \Omega \bar{a}_1. \tag{A2}$$

As z approaches a boundary point $t = a e^{i\alpha}$, the integral in (A2) is convergent in the principal value sense because the perturbation assumed in (A1) has satisfied $A(\zeta = t) = 0$. The boundary value of the contour integral in (A2) can be calculated using the Plemelj formula:

$$\left(\frac{1}{2\pi i} \int_L \frac{f(\zeta)}{\zeta - z} \, d\zeta \right)_{z \to t^{\pm}} = \pm \tfrac{1}{2} f(t) + \frac{1}{2\pi i} PV \int_L \frac{f(\zeta)}{\zeta - t} \, d\zeta \tag{A3}$$

where L is an arbitrary smooth curve or closed contour in the z plane and t lies along L. Plus $(+)$ and minus $(-)$ signs denote the left and right sides of L according to the direction of traversal. For the reference circle traversing in the anticlockwise direction, $(+)$ denotes the inclusion side while $(-)$ denotes the matrix side. The value of $A(\zeta)/(\zeta - z)$ as ζ and z approach t is equal to $A'(t) = A'(\alpha)/it$, where $A'(\alpha)$ is defined in (A1) for a given inclusion shape. It can then be shown that, as z approaches t from inside the inclusion,

$$\left(\frac{1}{2\pi i} \oint_{|\zeta|=a} \frac{A(\zeta)\zeta\bar{\Sigma}_1^0}{(\zeta - z)^2} \, d\zeta \right)_{z \to t^-} = -\tfrac{1}{2} i A'(\alpha) \bar{\Sigma}_1^0(\alpha) - \frac{1}{2\pi} \int_0^{2\pi} \frac{A(\theta)\bar{\Sigma}_1^0(\theta) e^{i(\theta - \alpha)}}{4 \sin^2[(\theta - \alpha)/2]} \, d\theta \tag{A4}$$

where the definition of the polar stress component $\hat{\Sigma}$ is given in (1) of the text. Substituting (A4) into (A2) gives the value of $\Phi_1'(t^+)$ along Γ. Repeating the same procedure one may calculate other relevant integrals that appear in calculating $\Phi_2'(t^-)$, $\Psi_1'(t^+)$ and $\Psi_2'(t^-)$. The stresses σ and $\hat{\Sigma}$ for the actual inclusion are written as

$$\sigma(\alpha) = \sigma^0(\alpha) + \delta\sigma(\alpha), \quad \hat{\Sigma}(\alpha) = \hat{\Sigma}^0(\alpha) + \delta\hat{\Sigma}(\alpha) \tag{A5}$$

where

$$\delta\sigma(\alpha) = 4 \operatorname{Re}[\Phi'(t)], \quad \delta\hat{\Sigma}(\alpha) = 2e^{2i\alpha}[\bar{t}\Phi''(t) + \Psi'(t)]. \tag{A6}$$

After some algebraic manipulation, the final solutions are found to be

$$\delta\sigma_1(\alpha) = -\Omega \operatorname{Re}\left\{ 2iA'(\alpha)\bar{\Sigma}_1^0(\alpha) + \frac{1}{2\pi} PV \int_0^{2\pi} A(\theta) \left(\frac{\bar{\Sigma}_1^0(\theta) e^{i(\theta - \alpha)}}{\sin^2[(\theta - \alpha)/2]} - \frac{4\Omega\hat{\Sigma}_1^0(\theta)}{1 - \Omega} \right) d\theta \right\}$$

$$\delta\sigma_2(\alpha) = \Pi \operatorname{Re}\left\{ -2iA'(\alpha)\bar{\Sigma}_2^0(\alpha) + \frac{1}{2\pi} PV \int_0^{2\pi} A(\theta) \frac{\bar{\Sigma}_2^0(\theta) e^{i(\theta - \alpha)}}{\sin^2[(\theta - \alpha)/2]} \, d\theta \right\}$$

$$\delta\hat{\Sigma}_1(\alpha) = iA'(\alpha)[\hat{\Sigma}_1^0(\alpha) - (1 + \Pi)\hat{\Sigma}_2^0(\alpha) - \Omega\bar{\Sigma}_1^0(\alpha)]$$
$$+ \frac{1}{2\pi} PV \int_0^{2\pi} A(\theta) \left[\frac{\hat{\Sigma}_1^0(\theta) e^{-i(\theta - \alpha)} - (1 + \Pi)\hat{\Sigma}_2^0(\theta) e^{-i(\theta - \alpha)} - \Omega\bar{\Sigma}_1^0(\theta) e^{i(\theta - \alpha)}}{2 \sin^2[(\theta - \alpha)/2]} - 2\Omega\bar{\Sigma}_1^0 \right] d\theta$$

$$\delta\hat{\Sigma}_2(\alpha) = iA'(\alpha)[\hat{\Sigma}_2^0(\alpha) - (1 + \Omega)\hat{\Sigma}_1^0(\alpha) - \Pi\bar{\Sigma}_2^0(\alpha)]$$
$$+ \frac{1}{2\pi} PV \int_0^{2\pi} A(\theta) \left[\frac{-\hat{\Sigma}_2^0(\theta) e^{-i(\theta - \alpha)} + (1 + \Omega)\hat{\Sigma}_1^0(\theta) e^{-i(\theta - \alpha)} + \Pi\bar{\Sigma}_2^0(\theta) e^{i(\theta - \alpha)}}{2 \sin^2[(\theta - \alpha)/2]} + \frac{2\Omega^2[\bar{\Sigma}_1^0(\theta) + \Omega\hat{\Sigma}_1^0(\theta)]}{1 - \Omega^2} \right] d\theta \tag{A7}$$

where $A(\theta)$ and $A'(\alpha)$ are given in (A1) for arbitrary inclusion shape $a(\theta)$. Once the deviatoric stress components $(\hat{\Sigma}_1^0, \hat{\Sigma}_2^0)$ are known along the boundary of the reference circular inclusion, one may immediately calculate the stress distribution along the actual inclusion boundary by (A7).

Nearly-circular holes

In the special case of a nearly-circular hole, we have $\Lambda = \Pi = -1$, $\hat{\Sigma}_1^0 = 0$ and $\hat{\Sigma}_2^0 = \sigma_{\theta\theta}^0$, where $\sigma_{\theta\theta}^0$ is the hoop stress distribution along the reference circular hole boundary. The general formulae (A7) reduce to

$$\delta\sigma_2 = -\frac{1}{2\pi} PV \int_0^{2\pi} \frac{A(\theta)\sigma_{\theta\theta}^0(\theta) \cos(\theta - \alpha)}{\sin^2[(\theta - \alpha)/2]} \, d\theta$$

$$\delta\hat{\Sigma}_2 = 2iA'(\alpha)\sigma_{\theta\theta}^0(\alpha) - \frac{1}{2\pi} PV \int_0^{2\pi} \frac{A(\theta)\sigma_{\theta\theta}^0(\theta) \cos(\theta - \alpha)}{\sin^2[(\theta - \alpha)/2]} \, d\theta \tag{A8}$$

which may be alternatively written as

$$\sigma_{rr}(\alpha) = 0, \quad \sigma_{r\theta}(\alpha) = A'(\alpha)\sigma^0_{\infty\theta}(\alpha), \quad \sigma_{\theta\theta} = \sigma^0_{\infty\theta} - \frac{1}{2\pi} PV \int_0^{2\pi} \frac{\sigma^0_{\infty\theta}(\theta)\cos(\theta-\alpha)}{\sin^2[(\theta-\alpha)/2]} \frac{a(\theta)-a(\alpha)}{a(\alpha)} \, d\theta. \tag{A9}$$

This solution matches a corresponding perturbation formula derived by Gao (1991b) in an earlier study on the stress concentration due to smooth polygon holes in an elastic sheet. In that work, Gao has used the perturbation formula (A9) to calculate the stress concentration at an elliptical hole subject to remote stresses and found good agreement between the perturbation result and the exact solution. In that case it was found that the error of (A9) is less than 5% for an aspect ratio of the ellipse as large as 1.5. The same range of accuracy is expected for the general perturbation formulae (A7) in the general case of bimaterial inclusion problems.

Nearly-circular disks

Equation (A7) can also be specialized to a nearly-circular disk by setting $\Delta = \Omega = -1$, $\hat{\Sigma}^0_2 = 0$ and $\hat{\Sigma}^0_1 = \sigma^0_{\infty\theta}$, where $\sigma^0_{\infty\theta}$ is interpreted as the hoop stress distribution along the boundary of the reference circular disk. It may be verified that the general formulae (A7) reduce to

$$\delta\sigma_1(\alpha) = \frac{1}{2\pi} PV \int_0^{2\pi} A(\theta)\sigma^0_{\infty\theta}(\theta)\left(\frac{\cos(\theta-\alpha)}{\sin^2[(\theta-\alpha)/2]} + 2\right) d\theta$$

$$\delta\hat{\Sigma}_1(\alpha) = 2iA'(\alpha) + \frac{1}{2\pi} PV \int_0^{2\pi} A(\theta)\sigma^0_{\infty\theta}(\theta)\left(\frac{\cos(\theta-\alpha)}{\sin^2[(\theta-\alpha)/2]} + 2\right) d\theta \tag{A10}$$

which may be alternatively written as

$$\sigma_{rr}(\alpha) = 0, \quad \sigma_{r\theta}(\alpha) = A'(\alpha)\sigma^0_{\infty\theta}(\alpha), \quad \sigma_{\theta\theta} = \sigma^0_{\infty\theta} + \frac{1}{2\pi} PV \int_0^{2\pi} \sigma^0_{\infty\theta}(\theta)\left(\frac{\cos(\theta-\alpha)}{\sin^2[(\theta-\alpha)/2]} + 2\right) \frac{a(\theta)-a(\alpha)}{a(\alpha)} \, d\theta. \tag{A11}$$

Slightly-undulating interfaces

Similar integral formulae may be written for a slightly-undulating bimaterial interface based on the general solution (60) and the Plemelj formula. Alternatively, one may consider a straight interface as a circular inclusion with infinite radius and an undulating interface as a special "nearly circular" inclusion. Along the undulating interface $y = A(x)$, the following integral formulae may be derived:

$$\delta\sigma_1(x) = -\Omega \, \mathrm{Re}\left\{2iA'(x)\Sigma^0_1(x) + \frac{2}{\pi} PV \int_{-\infty}^{\infty} \frac{\Sigma^0_1(t)[A(t)-A(x)]}{(t-x)^2} \, dt\right\}$$

$$\delta\sigma_2(x) = \Pi \, \mathrm{Re}\left\{-2iA'(x)\Sigma^0_2(x) + \frac{2}{\pi} PV \int_{-\infty}^{\infty} \frac{\Sigma^0_2(t)[A(t)-A(x)]}{(t-x)^2} \, dt\right\}$$

$$\delta\Sigma_1(x) = iA'(x)[\Sigma^0_1(x) - (1+\Pi)\Sigma^0_2(x) - \Omega\Sigma^0_1(x)] + \frac{1}{\pi} PV \int_{-\infty}^{\infty} \frac{\Sigma^0_1(t) - (1+\Pi)\Sigma^0_2(t) - \Omega\Sigma^0_1(t)}{(t-x)^2} [A(t)-A(x)] \, dt$$

$$\delta\Sigma_2(x) = iA'(x)[\Sigma^0_2(x) - (1+\Omega)\Sigma^0_1(x) - \Pi\Sigma^0_2(x)] + \frac{1}{\pi} PV \int_{-\infty}^{\infty} \frac{-\Sigma^0_2(t) + (1+\Omega)\Sigma^0_1(t) + \Pi\Sigma^0_2(t)}{(t-x)^2} [A(t)-A(x)] \, dt. \tag{A12}$$

In the special case of an undulating surface, the perturbation formula can be simplified by setting $\Lambda = \Pi = -1$, $\Sigma^0_1(x) = 0$ and $\Sigma^0_2(x) = -\sigma^0_{xx}(x)$, which leads to

$$\delta\sigma_2(x) = -\frac{2}{\pi} PV \int_{-\infty}^{\infty} \frac{\sigma^0_{xx}(t)[A(t)-A(x)]}{(t-x)^2} \, dt$$

$$\delta\Sigma_2(x) = 2iA'(x)\sigma^0_{xx}(x) - \frac{2}{\pi} PV \int_{-\infty}^{\infty} \frac{\sigma^0_{xx}(t)[A(t)-A(x)]}{(t-x)^2} \, dt. \tag{A13}$$

This is consistent with the solutions derived in Gao (1991a).